Supplemental Figure 1

A

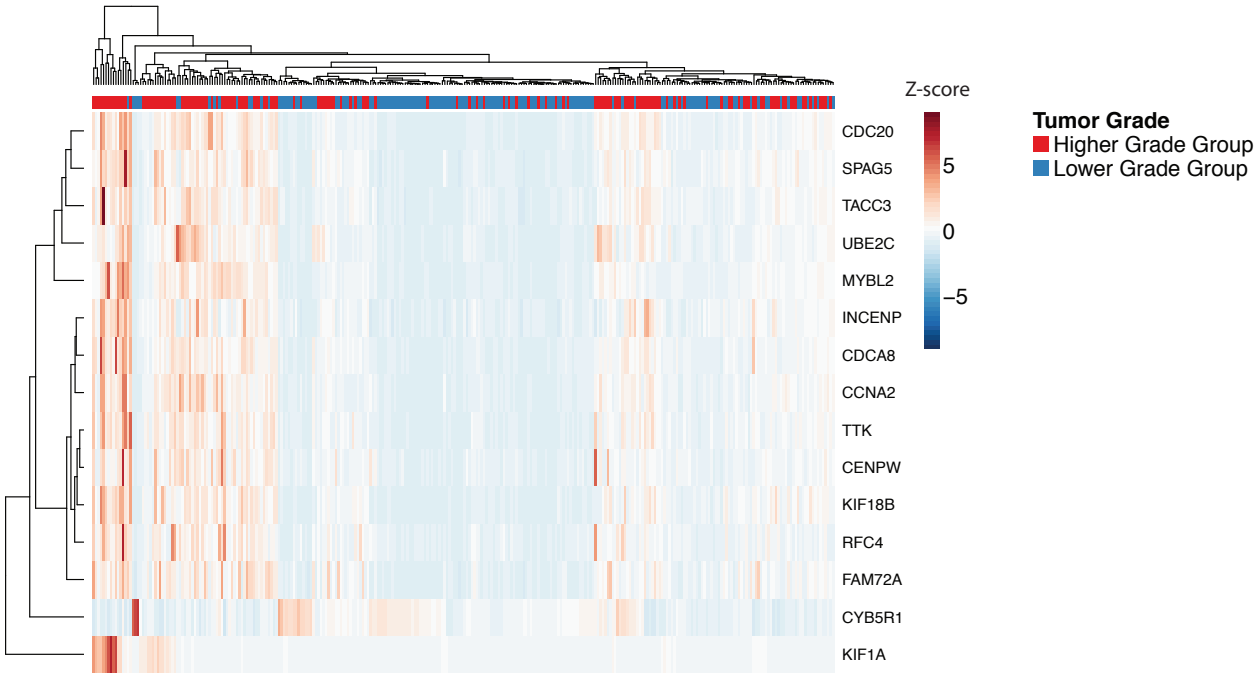

B

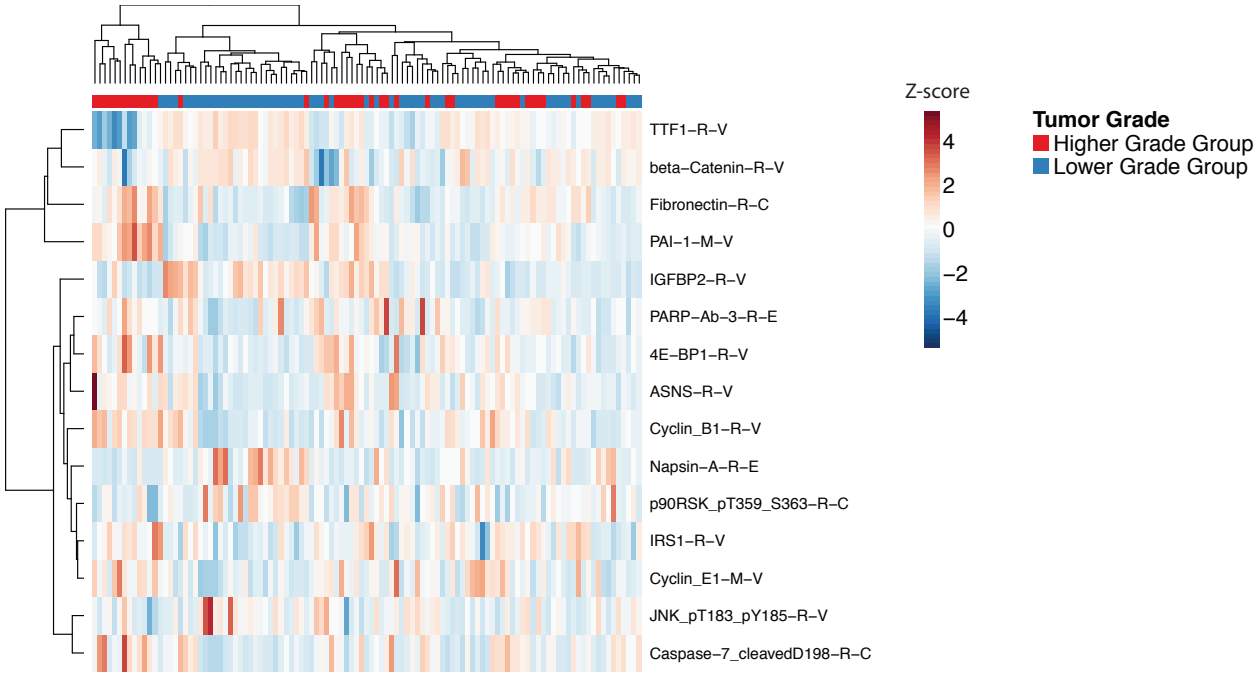

Supplemental Figure 1: Related to Figure 2. Heatmaps of gene expression or protein abundance associated with tumor differentiation status. (A) A heatmap showing the gene expression profiles associated with pathology grade. Patients were divided into a lower-grade group (with well or moderately differentiated tumor) and a higher-grade group (with poorly differentiated or moderate-to-poorly differentiated tumor). (B) A heatmap showing the protein abundance levels associated with pathology grade. Patients were divided into a lower-grade group and a higher-grade group as described above.

Supplemental Figure 2

A

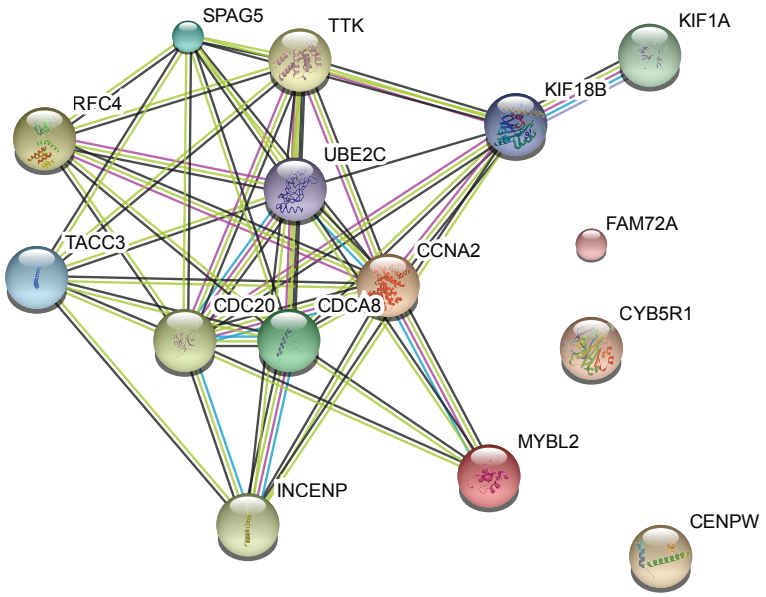

B

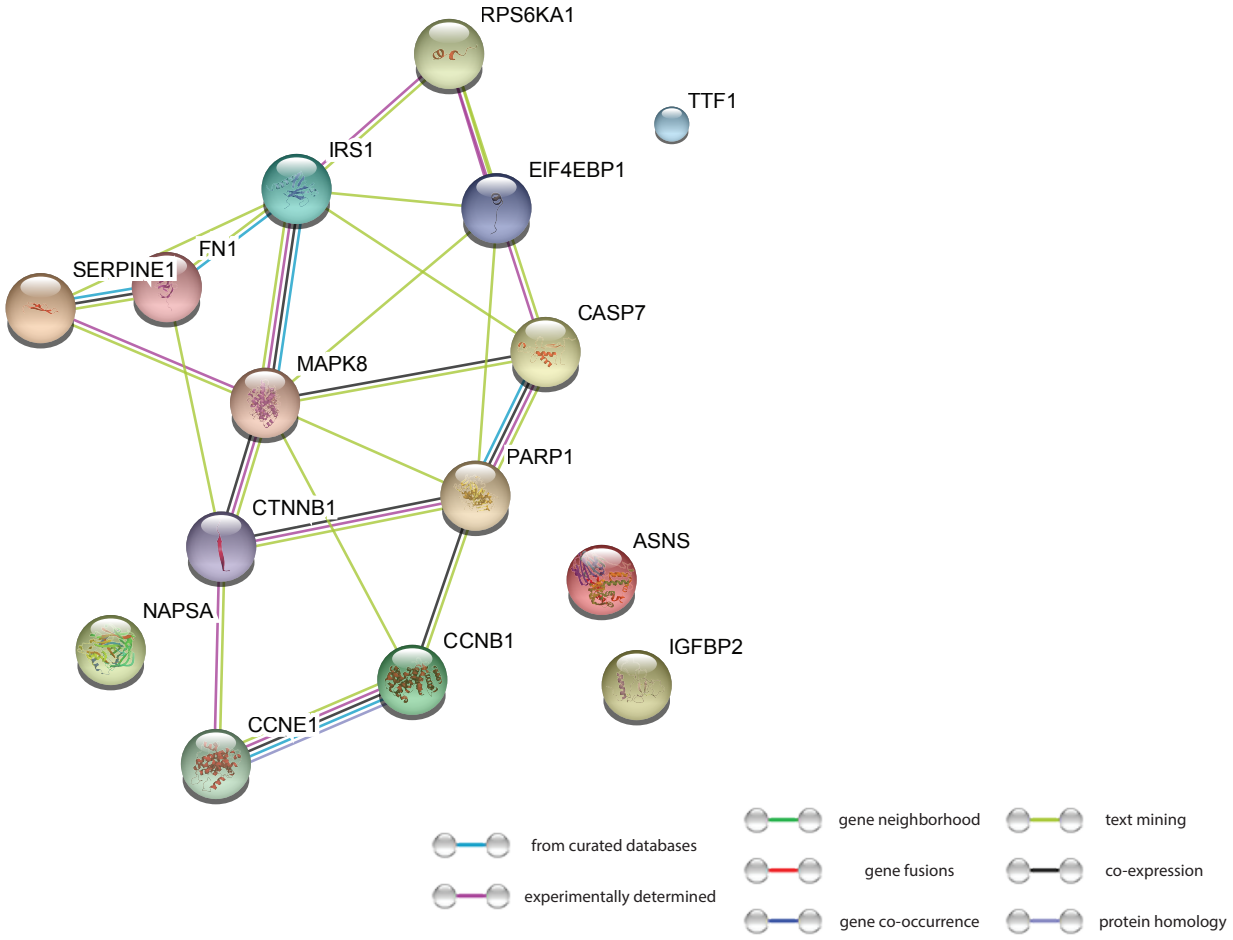

Supplemental Figure 2: Related to Figure 2. Transcriptomic and proteomic profiles are associated with patients' tumor grade. Both (A) transcriptomic and (B) proteomic features correlated with tumor grade formed tight interaction networks.

Supplemental Figure 3

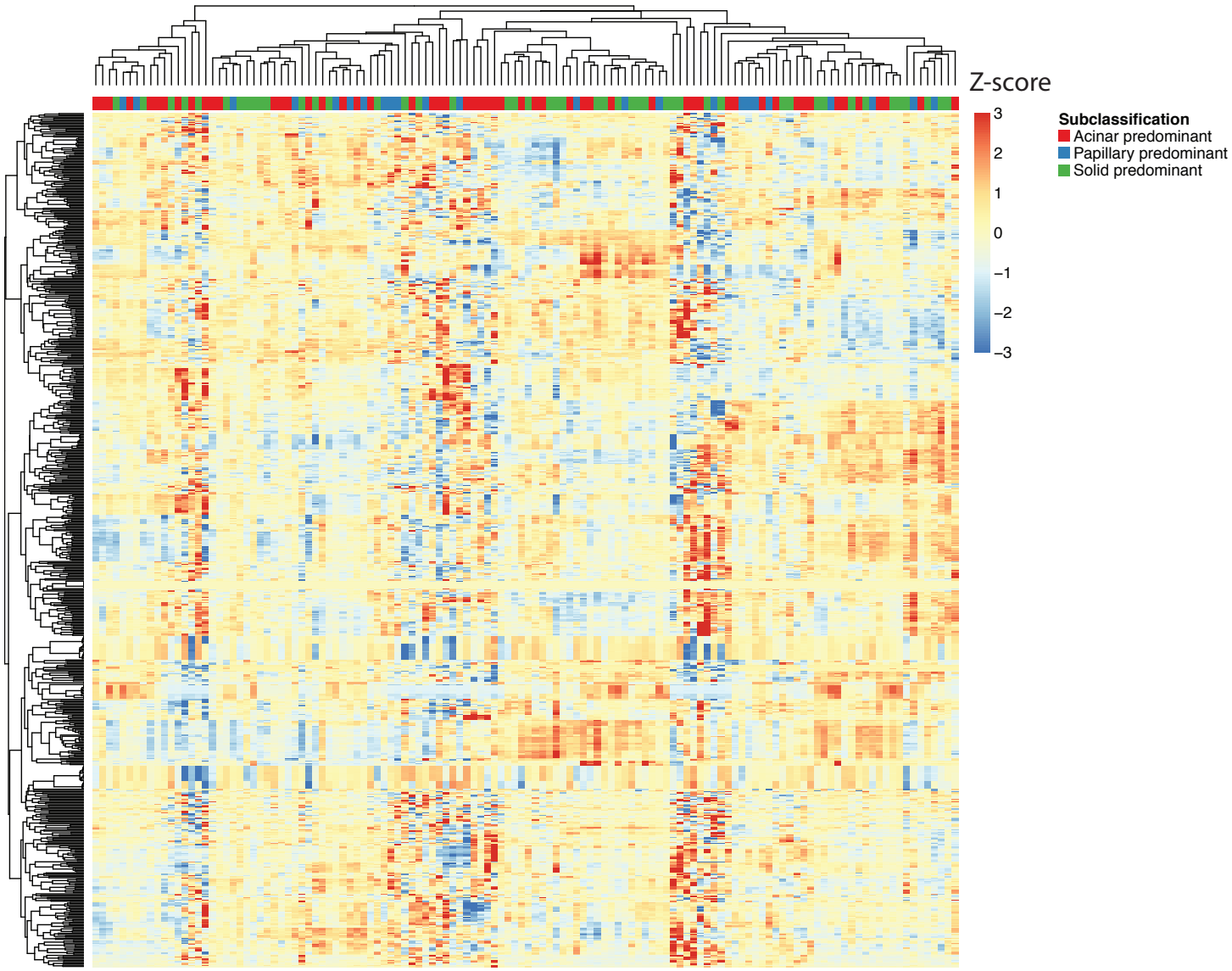

Supplemental Figure 3: Related to Figure 2. Clustering analysis of the quantitative histopathology image features. For better visualization, we selected three major lung adenocarcinoma sub-classifications that had more than 20 patients with available histopathology images.

Supplemental Figure 4

A

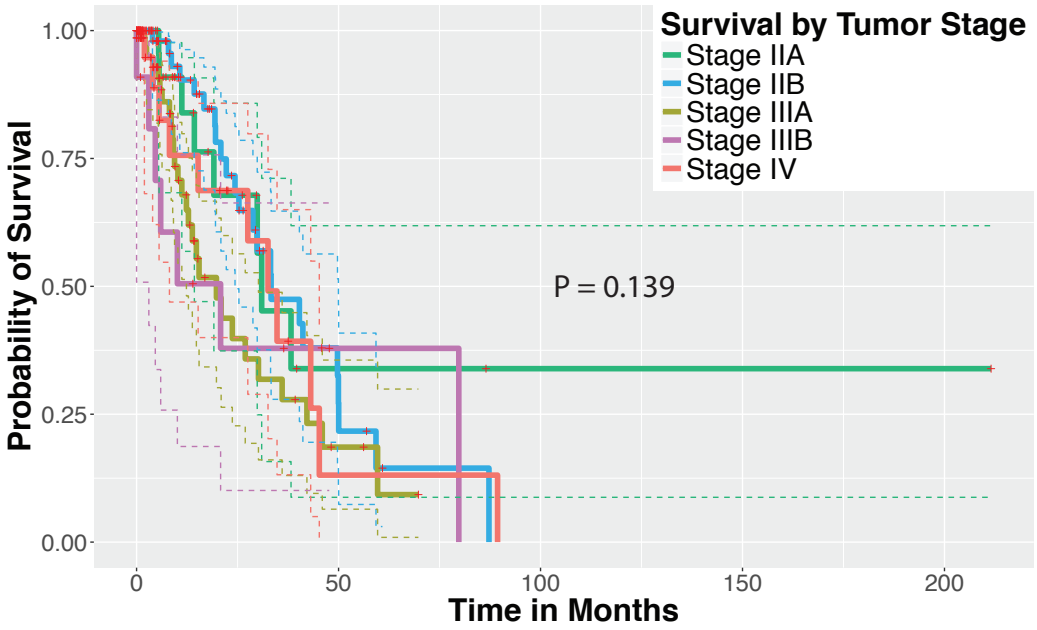

B

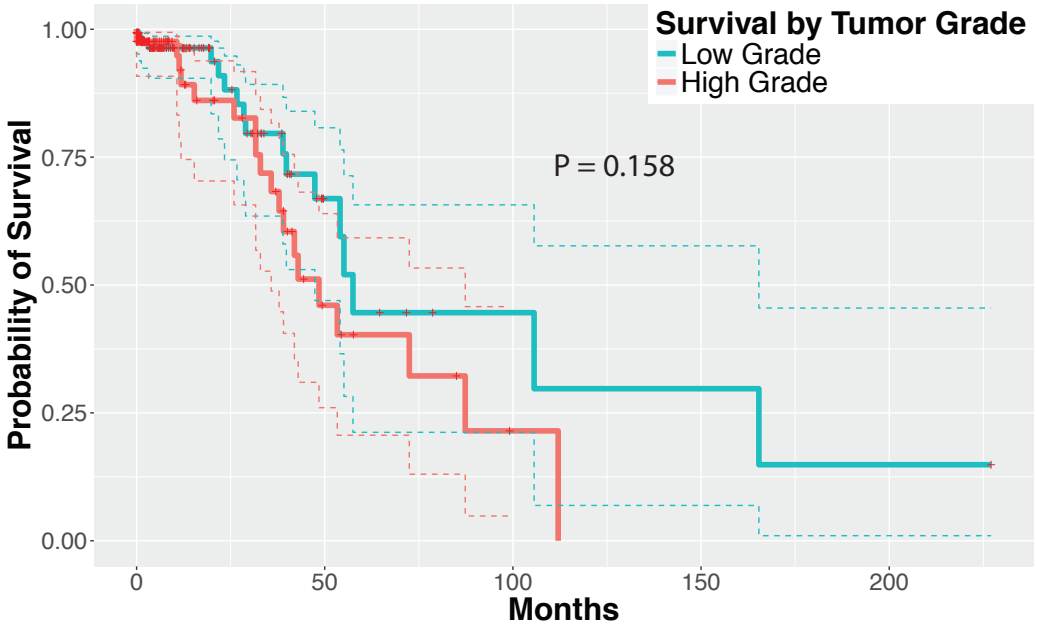

Supplemental Figure 4: Related to Figure 3. Additional survival prediction results using tumor stage and grade. Red asterisks indicated censored data. (A) Survival stratification of patients with stage II or higher lung adenocarcinoma. The differences in overall survival among lung adenocarcinoma patients with stage II or higher tumor was not significant in the TCGA cohort. Among stage IIa, IIb, IIIa, IIIb, and IV, the log-rank test P-value is 0.139. (B) Stage I lung adenocarcinoma patient survival stratified by binarized tumor grade (high-grade group versus low-grade group). Binarized grade alone could not predict patient survival reliably (log-rank test P = 0.158).

Supplemental Table 1: Related to Figure 1. Patient characteristics of The Cancer Genome Atlas (TCGA) cohort.

Characteristics	Summary
The Cancer Genome Atlas Cohort	N=538
Age	66.0 ± 9.9 years
Number of tumor histopathology image series	N=831
Number of histopathology image series of adjacent benign tissue	N=243
Number of histopathology image tiles	N=5,739,972
Grade	
Grade 1	62 (11.5 %)
Grade 1-2	11 (2.0 %)
Grade 2	180 (33.5 %)
Grade 2-3	39 (7.2 %)
Grade 3	170 (31.6 %)
Grade 4	5 (0.9 %)
Grade unavailable	71 (13.2 %)
Stage	
Stage I	254 (47.2 %)
Stage II	119 (22.1 %)
Stage III	81 (15.1 %)
Stage IV	25 (4.6 %)
Stage unavailable	59 (11.0 %)
TP53 Mutation	
Mutation	125 (23.2 %)
No mutation	105 (19.5 %)
BRAF Mutation	
Mutation with Known Clinical Significance	16 (3.0 %)
Mutation with Unknown Significance	6 (1.1 %)
No mutation	497 (92.3 %)
Data unavailable	19 (3.5 %)
EGFR Mutation	
Mutation with Known Clinical Significance	22 (4.1 %)
Mutation with Unknown Significance	11 (2.0 %)
No mutation	486 (90.3 %)
Data unavailable	19 (3.5 %)
MET Amplification	
Amplification	17 (3.2 %)
No amplification	498 (92.6 %)
Data unavailable	23 (4.3 %)

Supplemental Table 2: Related to Figure 1. Patient characteristics of stage I adenocarcinoma patients of The Cancer Genome Atlas (TCGA) and the Mayo Clinic cohorts.

Characteristics	Summary
Stage I Adenocarcinoma Patients in TCGA with Available Histopathology and Gene Expression Data	N = 222
Age	66.8 ± 9.5 years
Stage	
Stage IA	103 (46.4 %)
Stage IB	116 (52.3 %)
Stage I, IA or IB unspecified	3 (1.35 %)
Grade	
Grade 1	37 (16.7 %)
Grade 1-2	8 (3.60 %)
Grade 2	97 (43.7 %)
Grade 2-3	18 (8.11 %)
Grade 3	62 (27.9 %)
Survival outcomes	
Alive	185 (83.3 %)
Dead	37 (16.7 %)
Stage I Adenocarcinoma Patients in the Mayo Clinic Cohort	N = 27
Age	66.1 ± 12.6 years
Stage	
Stage IA	10 (37.0%)
Stage IB	17 (63.0 %)
Grade	
Grade 1	2 (7.4%)
Grade 2	18 (66.7%)
Grade 3	7 (25.9%)
Survival outcomes	
Alive	20 (74.1 %)
Dead	7 (25.9 %)

Supplemental Table 3: Related to Figure 2. Quantitative image features associated with TP53 mutation status.

Quantitative Image Features	Raw P-values	Adjusted P-values
Median_Cytoplasm_Intensity_LowerQuartileIntensity_MaskedEWithoutOverlap	5.54E-04	4.18E-02
Median_Cytoplasm_Intensity_MeanIntensityEdge_MaskedEWithoutOverlap	9.41E-04	4.18E-02
Median_Cytoplasm_Intensity_MeanIntensity_MaskedEWithoutOverlap	8.41E-04	4.18E-02
Median_Cytoplasm_Intensity_MedianIntensity_MaskedEWithoutOverlap	8.41E-04	4.18E-02
Median_Cytoplasm_Intensity_MinIntensityEdge_MaskedEWithoutOverlap	1.47E-04	4.18E-02
Median_Cytoplasm_Intensity_MinIntensity_MaskedEWithoutOverlap	5.65E-04	4.18E-02
Median_Cytoplasm_RadialDistribution_RadialCV_MaskedEWithoutOverlap_3of4	1.02E-04	4.18E-02
Median_FilteredNuclei_Intensity_LowerQuartileIntensity_MaskedEWithoutOverlap	7.20E-04	4.18E-02
Median_FilteredNuclei_Intensity_MeanIntensityEdge_MaskedEWithoutOverlap	9.61E-04	4.18E-02
Median_FilteredNuclei_Intensity_MeanIntensity_MaskedEWithoutOverlap	9.71E-04	4.18E-02
Median_FilteredNuclei_Intensity_MinIntensityEdge_MaskedEWithoutOverlap	1.93E-04	4.18E-02
Median_FilteredNuclei_Intensity_MinIntensity_MaskedEWithoutOverlap	3.45E-04	4.18E-02
Median_FilteredNuclei_RadialDistribution_RadialCV_MaskedEWithoutOverlap_3of4	2.61E-04	4.18E-02
Median_FilteredNuclei_Texture_AngularSecondMoment_MaskedHWithoutOverlap_3_0	6.69E-04	4.18E-02
Median_Nuclei_Intensity_IntegratedIntensityEdge_MaskedEWithoutOverlap	5.90E-04	4.18E-02
Median_Nuclei_Intensity_MinIntensityEdge_MaskedEWithoutOverlap	8.54E-04	4.18E-02
Median_FilteredNuclei_Texture_AngularSecondMoment_MaskedHWithoutOverlap_3_45	1.06E-03	4.31E-02
Median_Nuclei_Intensity_MeanIntensityEdge_MaskedEWithoutOverlap	1.15E-03	4.41E-02
Median_Cytoplasm_Intensity_UpperQuartileIntensity_MaskedEWithoutOverlap	1.35E-03	4.43E-02
Median_FilteredNuclei_Intensity_MedianIntensity_MaskedEWithoutOverlap	1.46E-03	4.43E-02
Median_FilteredNuclei_RadialDistribution_Ra	1.37E-03	4.43E-02

dialCV_MaskedEWithoutOverlap_4of4		
Median_FilteredNuclei_Texture_Entropy_MaskedHWithoutOverlap_3_135	1.46E-03	4.43E-02
Median_Nuclei_Intensity_MinIntensity_MaskedEWithoutOverlap	1.48E-03	4.43E-02
Median_Cytoplasm_RadialDistribution_RadialCV_MaskedEWithoutOverlap_4of4	1.60E-03	4.59E-02
Median_Nuclei_Intensity_LowerQuartileIntensity_MaskedEWithoutOverlap	1.68E-03	4.63E-02
Median_FilteredNuclei_Texture_Entropy_MaskedHWithoutOverlap_3_0	1.78E-03	4.72E-02
Median_Nuclei_Intensity_MeanIntensity_MaskedEWithoutOverlap	1.94E-03	4.96E-02

Supplemental Table 4: Related to Figure 2. KEGG pathway enrichments for genes associated with TP53 mutation status in lung adenocarcinoma.

ID	Term	Number of Genes	Adjusted P-value
4110	Cell cycle	29	2.07E-10
3030	DNA replication	11	7.68E-05
3460	Fanconi anemia pathway	11	2.84E-03
3430	Mismatch repair	7	5.95E-03
3440	Homologous recombination	7	1.45E-02
4115	p53 signaling pathway	11	1.63E-02

Supplemental Table 5: Related to Figure 2. Quantitative image features associated with lung adenocarcinoma sub-classifications and those achieved marginal significance in the association.

Quantitative Image Features	Raw P-values	Adjusted P-values
Median_Nuclei_Texture_AngularSecondMoment_MaskedHWithoutOverlap_3_0	3.66E-05	2.54E-02
Median_FilteredNuclei_RadialDistribution_RadialCV_MaskedEWithoutOverlap_4of4	4.00E-04	5.37E-02
Median_Nuclei_RadialDistribution_RadialCV_MaskedEWithoutOverlap_4of4	3.54E-04	5.37E-02
Median_Nuclei_RadialDistribution_RadialCV_MaskedHWithoutOverlap_3of4	4.17E-04	5.37E-02
Median_Nuclei_Texture_AngularSecondMoment_MaskedHWithoutOverlap_3_135	4.64E-04	5.37E-02
Median_Nuclei_Texture_AngularSecondMoment_MaskedHWithoutOverlap_3_45	1.73E-04	5.37E-02

Supplemental Table 6: Related to Figure 2. Quantitative image features associated with purity of lung adenocarcinoma tissue.

Quantitative Image Features	Raw P-values	Adjusted P-values
Median_Nuclei_Texture_AngularSecondMoment_MaskedHWithoutOverlap_3_135	5.11E-05	1.76E-02
Median_Nuclei_Texture_InverseDifferenceMoment_MaskedHWithoutOverlap_3_135	2.83E-05	1.76E-02
Median_FilteredNuclei_Texture_Contrast_MaskedEWithoutOverlap_3_0	1.41E-04	1.83E-02
Median_FilteredNuclei_Texture_DifferenceEntropy_MaskedEWithoutOverlap_3_0	1.86E-04	1.83E-02
Median_FilteredNuclei_Texture_DifferenceVariance_MaskedEWithoutOverlap_3_45	1.15E-04	1.83E-02
Median_Nuclei_Texture_AngularSecondMoment_MaskedHWithoutOverlap_3_90	1.44E-04	1.83E-02
Median_Nuclei_Texture_Entropy_MaskedHWithoutOverlap_3_90	1.86E-04	1.83E-02
Median_FilteredNuclei_Texture_AngularSecondMoment_MaskedHWithoutOverlap_3_0	3.03E-04	2.11E-02
Median_Nuclei_Texture_AngularSecondMoment_MaskedHWithoutOverlap_3_45	2.77E-04	2.11E-02
Median_Nuclei_Texture_Entropy_MaskedHWithoutOverlap_3_135	3.06E-04	2.11E-02
Median_FilteredNuclei_Texture_InverseDifferenceMoment_MaskedEWithoutOverlap_3_0	3.99E-04	2.28E-02
Median_Nuclei_AreaShape_Solidity	3.86E-04	2.28E-02
Median_Nuclei_Texture_AngularSecondMoment_MaskedHWithoutOverlap_3_0	4.31E-04	2.28E-02
Median_FilteredNuclei_Texture_DifferenceEntropy_MaskedEWithoutOverlap_3_45	4.75E-04	2.34E-02
Median_Cytoplasm_RadialDistribution_FracAtD_MaskedEWithoutOverlap_1of4	7.14E-04	2.50E-02
Median_FilteredNuclei_AreaShape_Zernike_5_3	9.56E-04	2.50E-02
Median_FilteredNuclei_Texture_AngularSecondMoment_MaskedHWithoutOverlap_3_135	6.63E-04	2.50E-02
Median_FilteredNuclei_Texture_AngularSecondMoment_MaskedHWithoutOverlap_3_90	7.60E-04	2.50E-02
Median_FilteredNuclei_Texture_Contrast_MaskedEWithoutOverlap_3_45	9.76E-04	2.50E-02
Median_FilteredNuclei_Texture_Contrast_MaskedEWithoutOverlap_3_90	8.71E-04	2.50E-02
Median_FilteredNuclei_Texture_Correlation_MaskedEWithoutOverlap_3_0	9.66E-04	2.50E-02

Median_FilteredNuclei_Texture_Entropy_MaskedHWithoutOverlap_3_0	8.80E-04	2.50E-02
Median_FilteredNuclei_Texture_InverseDifferenceMoment_MaskedHWithoutOverlap_3_135	1.02E-03	2.50E-02
Median_Nuclei_AreaShape_Extent	7.77E-04	2.50E-02
Median_Nuclei_AreaShape_FormFactor	7.68E-04	2.50E-02
Median_Nuclei_RadialDistribution_RadialCV_MaskedHWithoutOverlap_2of4	9.86E-04	2.50E-02
Median_Nuclei_Texture_Entropy_MaskedHWithoutOverlap_3_45	6.56E-04	2.50E-02
Median_Nuclei_Texture_InverseDifferenceMoment_MaskedHWithoutOverlap_3_0	9.66E-04	2.50E-02
Median_FilteredNuclei_Texture_Entropy_MaskedHWithoutOverlap_3_90	1.39E-03	3.31E-02
Median_FilteredNuclei_Texture_DifferenceEntropy_MaskedHWithoutOverlap_3_45	1.48E-03	3.40E-02
Median_FilteredNuclei_Texture_DifferenceEntropy_MaskedHWithoutOverlap_3_135	1.70E-03	3.66E-02
Median_Nuclei_Texture_DifferenceEntropy_MaskedHWithoutOverlap_3_135	1.68E-03	3.66E-02
Median_FilteredNuclei_Texture_Contrast_MaskedHWithoutOverlap_3_135	1.84E-03	3.70E-02
Median_FilteredNuclei_Texture_DifferenceVariance_MaskedEWithoutOverlap_3_0	1.90E-03	3.70E-02
Median_Nuclei_Texture_Entropy_MaskedHWithoutOverlap_3_0	1.79E-03	3.70E-02
Median_Nuclei_Texture_InverseDifferenceMoment_MaskedHWithoutOverlap_3_45	1.93E-03	3.70E-02
Median_FilteredNuclei_AreaShape_Solidity	2.21E-03	3.91E-02
Median_FilteredNuclei_Texture_AngularSecondMoment_MaskedHWithoutOverlap_3_45	2.17E-03	3.91E-02
Median_FilteredNuclei_Texture_Correlation_MaskedEWithoutOverlap_3_45	2.11E-03	3.91E-02
Median_FilteredNuclei_Texture_DifferenceEntropy_MaskedHWithoutOverlap_3_0	2.44E-03	4.00E-02
Median_FilteredNuclei_Texture_InverseDifferenceMoment_MaskedEWithoutOverlap_3_90	2.39E-03	4.00E-02
Median_Nuclei_Texture_Contrast_MaskedHWithoutOverlap_3_135	2.32E-03	4.00E-02
Median_FilteredNuclei_Texture_Entropy_MaskedHWithoutOverlap_3_135	2.63E-03	4.12E-02
Median_Nuclei_Texture_Contrast_MaskedHWithoutOverlap_3_45	2.63E-03	4.12E-02
Median_FilteredNuclei_RadialDistribution_Fr	2.88E-03	4.31E-02

acAtD_MaskedEWithoutOverlap_2of4		
Median_Nuclei_RadialDistribution_FracAtD_MaskedEWithoutOverlap_2of4	2.87E-03	4.31E-02
Median_FilteredNuclei_Texture_Correlation_MaskedEWithoutOverlap_3_135	2.95E-03	4.32E-02
Median_Cytoplasm_Texture_SumEntropy_MaskedEWithoutOverlap_3_90	3.30E-03	4.33E-02
Median_FilteredNuclei_AreaShape_Zernike_9_7	3.18E-03	4.33E-02
Median_FilteredNuclei_Texture_DifferenceEntropy_MaskedEWithoutOverlap_3_90	3.36E-03	4.33E-02
Median_FilteredNuclei_Texture_DifferenceVariance_MaskedEWithoutOverlap_3_90	3.12E-03	4.33E-02
Median_FilteredNuclei_Texture_DifferenceVariance_MaskedHWithoutOverlap_3_45	3.40E-03	4.33E-02
Median_FilteredNuclei_Texture_InfoMeas1_MaskedEWithoutOverlap_3_0	3.18E-03	4.33E-02
Median_Nuclei_RadialDistribution_FracAtD_MaskedEWithoutOverlap_3of4	3.27E-03	4.33E-02
Median_Nuclei_Texture_DifferenceEntropy_MaskedHWithoutOverlap_3_45	3.49E-03	4.37E-02
Median_FilteredNuclei_Texture_DifferenceEntropy_MaskedEWithoutOverlap_3_135	3.59E-03	4.42E-02
Median_Cytoplasm_Texture_SumEntropy_MaskedEWithoutOverlap_3_135	4.01E-03	4.65E-02
Median_FilteredNuclei_Texture_Contrast_MaskedHWithoutOverlap_3_45	3.87E-03	4.65E-02
Median_Nuclei_RadialDistribution_FracAtD_MaskedEWithoutOverlap_4of4	4.05E-03	4.65E-02
Median_Nuclei_Texture_InverseDifferenceMoment_MaskedHWithoutOverlap_3_90	3.94E-03	4.65E-02
Median_Cytoplasm_Texture_SumVariance_MaskedEWithoutOverlap_3_90	4.16E-03	4.67E-02
Median_FilteredNuclei_Texture_DifferenceVariance_MaskedEWithoutOverlap_3_135	4.20E-03	4.67E-02
Median_FilteredNuclei_AreaShape_FormFactor	4.56E-03	4.83E-02
Median_FilteredNuclei_Texture_InverseDifferenceMoment_MaskedEWithoutOverlap_3_135	4.56E-03	4.83E-02
Median_FilteredNuclei_Texture_InverseDifferenceMoment_MaskedHWithoutOverlap_3_0	4.56E-03	4.83E-02
Median_FilteredNuclei_RadialDistribution_FracAtD_MaskedEWithoutOverlap_4of4	4.85E-03	4.92E-02
Median_Nuclei_Texture_SumAverage_Masked	4.77E-03	4.92E-02

EWithoutOverlap_3_0		
Median_Nuclei_Texture_SumAverage_MaskedEWithoutOverlap_3_135	4.81E-03	4.92E-02